LIGO Laboratory / LIGO Scientific Collaboration

LIGO-T040136-00-K

Advanced LIGO UK

June 2004

Measurement of shadow-sensor displacement sensitivities

N Lockerbie, Strathclyde

Distribution of this document:
Inform aligo_sus

This is an internal working note
of the Advanced LIGO Project, prepared by members of the UK team.

Institute for Gravitational Research
University of Glasgow
University Avenue, Glasgow G12 8QQ,
Scotland UK

+44 (0) 131 440 5880

Department of Physics
University of Birmingham

+44 (0) 121 414 6447

Engineering Department
CCLRC Rutherford Appleton Laboratory
Chilton, Didcot, Oxon OX12 0NA
Phone +44 (0) 1235 44 5297
Fax +44 (0) 1235 445843

Particle Physics and Astronomy Research Council (PPARC)

http://www.ligo.caltech.edu/

http://www.eng-external.rl.ac.uk/advligo/papers_public/ALUK_Homepage.htm.

UNIVERSITY OF STRATHCLYDE

Measurement of shadow-sensor displacement sensitivities

At present there are two main issues concerning the LIGO hybrid OSEM type of shadow-sensor: its small span (currently ~ 0.7 mm), and its sensitivity (currently ~ 3×10^{-10} m/rt-Hz). These are both somewhat marginal in the context of Advanced LIGO.

These issues have been explored over the past 2 weeks through three parallel investigations: -

- increasing the shadow-sensor span through the use of different Flag geometries
- looking into the source of the excess noise in shadow-sensor systems
- increasing the span and reducing the noise through the use of different emitter-detector pairs.

Different Flag geometries

Figure1. From the left: 2 mm dia. 5 mm long LIGO hybrid OSEM Flag (uppermost part of stack), a 4 mm dia. Flag with a 1:6 taper, and a 2.5 mm and a 4.0 mm dia. Flag, both with a 1:3 taper. A spherical-ended 3.25 mm dia. Flag (not shown) has also been machined. This has been used for the measurements on the twelve different emitter-detector pairs, described below in Tables 3(a) and (b).

These Flags were used together with the Honeywell SME2470 infrared LED emitter, and the Honeywell SMD2420 photodiode detector—both mounted in the LIGO hybrid OSEM—in order to try and extend the sensing span beyond its current value of 0.7 mm.

The concept was found to work, a 1:6 taper increasing the sensing span out to 4 mm, as shown in Fig.2. As anticipated, the maximum (absolute) value of the slope of the output voltage vs Flag position was found to fall—here by a factor close to 6 (6.44).

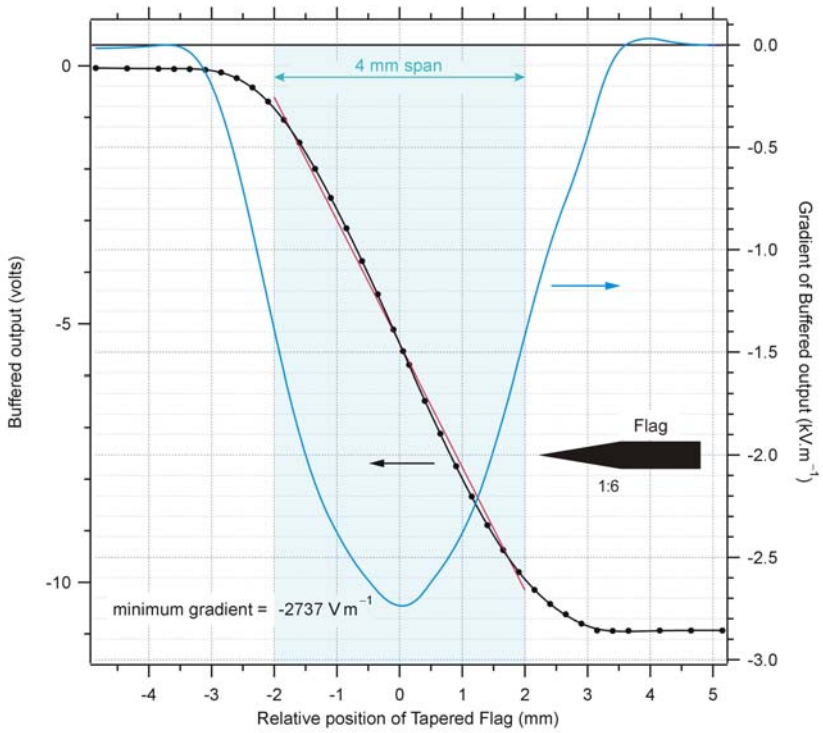

Figure 2. Data taken using the Honeywell emitter-detector pair SME2470-SMD2420 mounted within the LIGO hybrid OSEM. Left ordinate (data points and black line interpolation fit): buffered output voltage as a function tapered Flag position. Right ordinate: slope of the interpolation fit.

The source of the excess noise in shadow-sensor systems

The level of shot noise was estimated for the shadow sensor in the LIGO hybrid OSEM. At a detected photocurrent level of 34.6 μA, as obtained with this shadow-sensor, the detector's shot

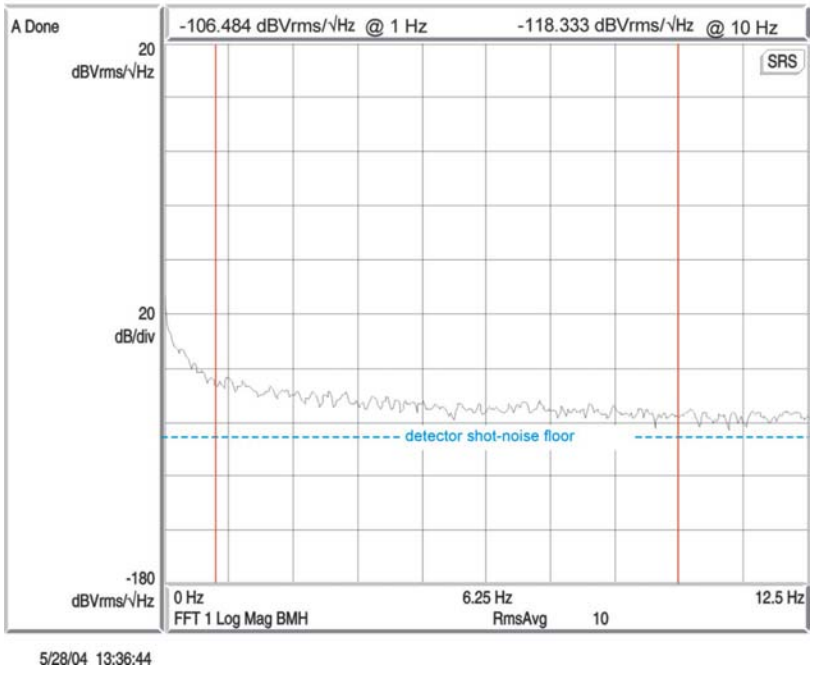

Figure3. The detector's shot noise floor was at –125.48 dBVrms/$\sqrt{Hz}$. The noise spectrum here was obtained using an AD743 'transconductance' op-amp.

noise should be at the level of –125.48 dBVrms/$\sqrt{\text{Hz}}$. This level, shown in Fig.3, lies typically 19 dB below the measured noise level for the system at 1 Hz. As the calculated noise contribution at 1 Hz from the AD743 'transconductance' op-amp used here is around 20 dB *below* the shot noise limit, its noise contribution is quite negligible, here.

Therefore, I concluded that the emitter-detector pair contributed around 19 dB Vrms/$\sqrt{\text{Hz}}$ of excess noise at 1 Hz (7 dB Vrms/$\sqrt{\text{Hz}}$ at 10 Hz); and, with approximately ±1 dB uncertainty in each of these figures, this noise could very well have been 'pink' in nature, with a '1/f' Power Spectral Density (investigation over a wider bandwidth could confirm this). Thus, it seemed that at 1 Hz the Honeywell emitter-detector pair were generating noise at a power level approximately two orders of magnitude above the shot noise limit.

In order to arrive at the AD743 as a suitable 'transconductance' amplifier for this work a number of op-amps were investigated, and this number was pruned down to leave a short-list of eight, as shown in the table below. The voltage noise at the output of each of these op-amps was then calculated using a spreadsheet for the following conditions

- A 'transconductance' configuration was assumed with a 160k feedback resistor—as used with the LIGO hybrid OSEM.
- An ambient temperature of 300 K was used.
- The voltage noise at 1 Hz was derived from that given at 10 Hz in the data sheets using a 1/f PSD extrapolation from the given voltage noise plot, or a 1/f PSD extrapolation to 1 Hz from either the voltage noise level given at 10 Hz, or from the intersection of the voltage noise level at 1 kHz together with the 1/f corner frequency (or 80 Hz, if this were not given).
- The current noise at 1 Hz was derived from that given at 10 Hz using a 1/f PSD extrapolation from the given current noise plot, or a 1/f PSD extrapolation to 1 Hz from either the current noise level given at 10 Hz, or from the intersection of the current noise level at 1 kHz together with the stated 1/f corner frequency (or 140 Hz, if this were not given). If no current noise level were given then the shot noise from the op-amp's input bias current was assumed. This noise current was assumed to flow in the 160k feedback resistor.
- 'Typical' parameter values from the data sheets were used.

The op-amp list was then ordered according to the final output noise level. The arrowed op-amp in the list (the LT1125) is seen to be significantly poorer than the AD743 for this particular value of feedback resistor. This particular op-amp is the (quad) type used in the LIGO 'Satellite amplifier' for the hybrid OSEMs. However, the list order would certainly change if it were possible to employ a lower value of feedback resistor than the 160k assumed here.

Total noise @ 1 Hz (Vrms/$\sqrt{\text{Hz}}$)	Op-amp	type
5.92E-08	AD743	biFET
6.34E-08	LT1793	JFET
1.04E-07	AD795	FET
1.96E-07	OP07	bipolar
3.24E-07	AD797	bipolar
3.36E-07	AD8512	JFET
8.02E-07	OP27	bipolar
1.60E-06	→ LT1125	bipolar

Several experiments were carried out in order to try and discover if the major source of the excess noise was the infrared LED (SME2470), the photodiode (SMD2420), or, perhaps, both.

Firstly, a BPW34S photodiode and a Honeywell SMD2420 photodiode were separately illuminated by the same Honeywell SME2470 infrared LED. In each case the distance from the LED to the respective detector was adjusted to give closely the same photocurrent (34.8 μA). The noise power spectra were then obtained for the two detectors under conditions of constant current (34.8 mA) through the LED. The measured noise levels were

SMD2420:	-105.634 dBVrms/rt-Hz @ 1 Hz	-120.688 dBVrms/rt-Hz @ 10 Hz
BPW34S:	-105.000 dBVrms/rt-Hz @ 1 Hz	-119.966 dBVrms/rt-Hz @ 10 Hz.

Given the ±1 dB uncertainty in these measurements, these two very different photodiode detectors were remarkably similar, given their very different physical construction, in their apparent level of intrinsic noise (or lack of it).

Secondly, two nominally identical (matched) BPW34S photodiodes were mounted side-by-side, close together on the same substrate. They were illuminated by a single Honeywell SME2470 infrared LED, this being powered by a constant current source (34.8 mA). One photodiode, then the other, then both together (in parallel), were connected to the AD743 transconductance amplifier. In each case the distance from the LED to the respective detector(s) was adjusted to give closely the same photocurrent (34.8 μA). The noise power spectra were then obtained for the three cases. The measured noise levels were

BPW34S #1:	-106.738 dBVrms/rt-Hz @ 1 Hz	-117.443 dBVrms/rt-Hz @ 10 Hz
BPW34S #2:	-105.907 dBVrms/rt-Hz @ 1 Hz	-116.439 dBVrms/rt-Hz @ 10 Hz
BPW34S #1 and 2:	-106.950 dBVrms/rt-Hz @ 1 Hz	-117.553 dBVrms/rt-Hz @ 10 Hz.

Once again these results are remarkably similar. There was no sign of statistically independent excess noise fluctuations leading to a measurably lower noise in the paralleled detectors.

Thirdly, two Honeywell SME2470 infrared LEDs were used to illuminate a single BPW34S photodiode. Two separate current sources (34.8 mA, each) were used to power the two emitters. The distance of each LED from the photodiode was adjusted until they gave equal contributions to the net photocurrent of 34.8 μA. The LEDs were then found to be at approximately 38 and 40 mm from the photodiode, respectively. The noise power spectrum was measured. Then the LEDs were used separately to illuminate the detector, the distance being shortened as appropriate in order to bring the photocurrent back to 34.8 μA. The noise power spectrum was measured in each case. The measured noise levels were

SME2470 #1:	-101.817 dBVrms/rt-Hz @ 1 Hz	-115.883 dBVrms/rt-Hz @ 10 Hz
SME2470 #2:	-100.551 dBVrms/rt-Hz @ 1 Hz	-112.691 dBVrms/rt-Hz @ 10 Hz
SME2470 #1 and 2:	-103.736 dBVrms/rt-Hz @ 1 Hz	-112.593 dBVrms/rt-Hz @ 10 Hz

These noise levels were all rather higher than those measured before, but there was perhaps just a suggestion—one reinforced by measurements reported below—that at 1 Hz a pair of independent LEDs was less noisy than each LED taken on its own, for a given level of photocurrent in the detector. At this point a shadow of suspicion had fallen on the Honeywell LEDs.

And finally, the following experiment was carried out using a single Honeywell emitter-detector pair. A simple light-pipe was constructed from a 46 mm length of thin-walled brass tube, having an i.d. of 2.6 mm. This tube was highly-polished, internally, and its ends were insulated electrically with a thin coat of epoxy resin, and small paper disks. The insulation was necessary

in order to avoid shorting out the electrodes of the surface-mount ceramic chip emitter and detector.

(a)

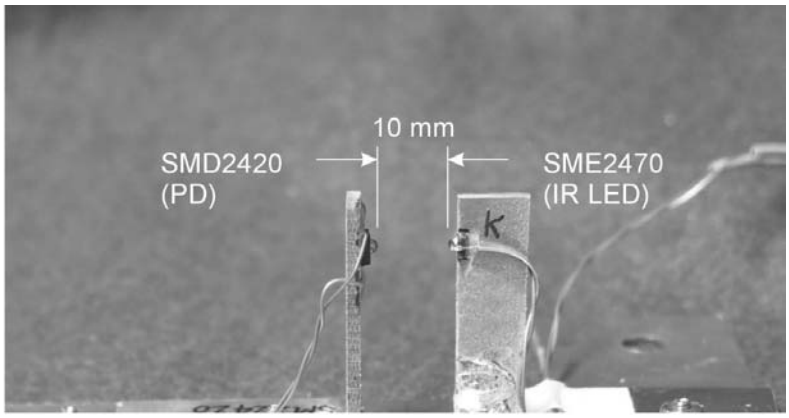

(b)

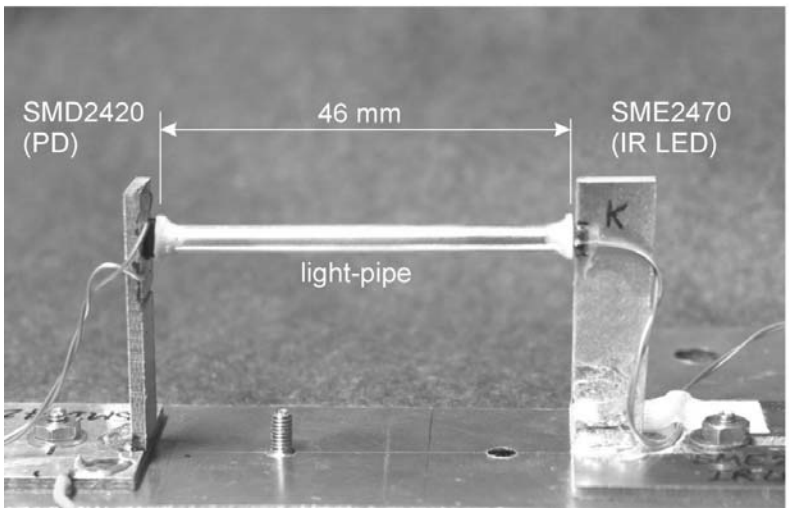

Figure 4. The same infrared emitter-detector pair was used in both (a) and (b), the constant current flowing through the Honeywell SME2470 infrared LED emitter being 34.8 mA in both cases. In (b) the emitter and detector were linked by a highly reflective (polished brass) light-pipe, of 2.6 mm internal diameter. The photocurrent induced in the Honeywell SMD2420 photodiode (PD) by the infrared radiation from the LED was then arranged—by varying the LED-to-photodiode distance in (a)—to be closely the same in (a) and (b), i.e.33.9 μA at 10 mm distance in (a), and 34.2 μA at 46 mm distance via the light-pipe, in (b).

However, over three noise measurements at each distance the noise level at 1 Hz was found to be measurably lower in (b) than in (a), as shown in Fig.5, the difference being 3.5 ± 2 dB. During the noise measurements the light-pipe was connected electrically to ground.

One explanation for this result is that at 1 Hz different regions of the LED chip are 'twinkling' on and off in such a way that the infrared emission is varying somewhat in *direction* as time elapses, thereby contributing to noise in (a), but not in (b). Note that a temporal variation alone in the emitted infrared energy flux would have led to no difference in the measured noise levels in (a) and (b). This effect may be being exacerbated by the very short focal length of the SME2470's lens, together with the finite size of its underlying LED chip (0.32 mm × 0.25 mm).

- In summary, the SME2470 infrared LED appears to be a strong candidate for much of the measured excess noise at 1 Hz in the LIGO hybrid OSEM.

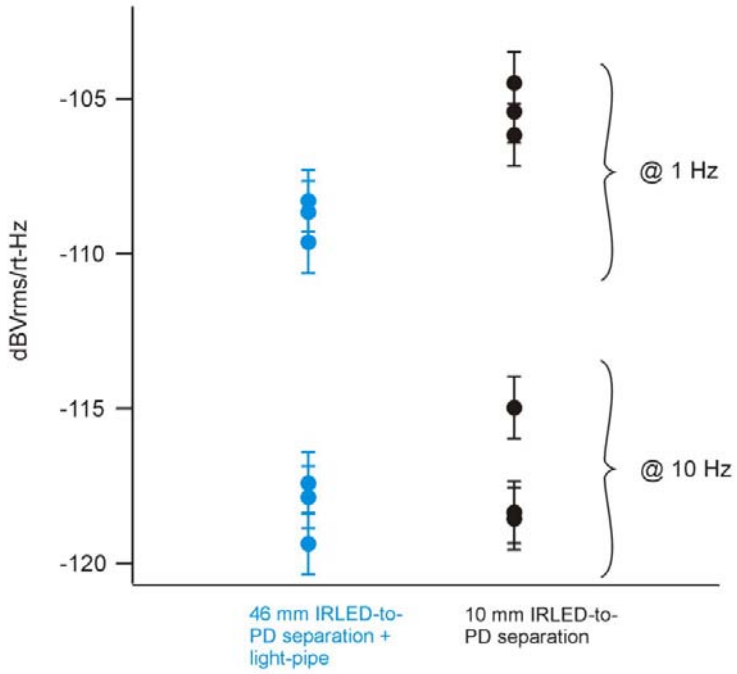

Figure 5. Repeated noise measurements for the Honeywell SME2470 IRLED - SMD2420 PD pair. At 1 Hz the noise was lower when the emitter-detector pair were connected together optically by a 46 mm long light-pipe, than by an unconstrained 10 mm gap.

Nevertheless, the optical quality of the LED seems to be good, with the rectangular infrared image of the chip itself being just discernible on a sensitive screen, as shown in Fig.6.

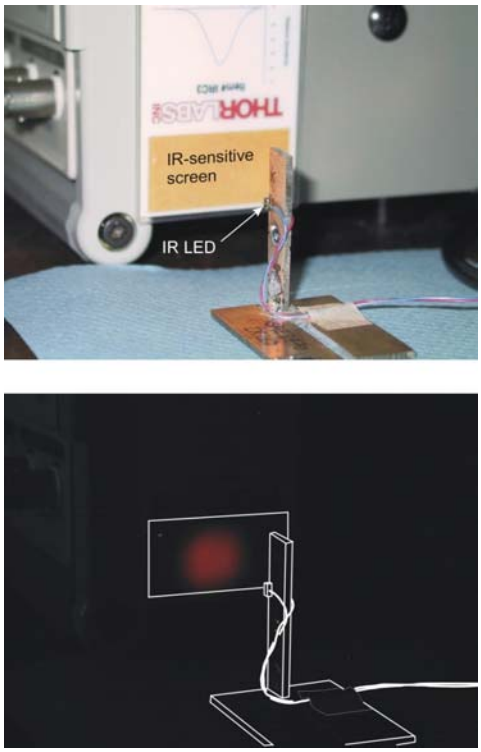

Figure 6. Upper view with the lab lights on: Honeywell SME2470 infrared LED pointing at an infrared-sensitive screen. Lower view: lab lights off, showing the dull-orange coloured essentially rectangular-section beam pattern on the screen. The LED-to-screen distance was approximately 33 mm.

Span and noise in different emitter-detector pairs

Two mounting jigs to take the shadow-sensor emitters and detectors in Tables 1 and 2 were designed and machined, so that they could be mounted, facing each other, on an XY micrometer stage, as shown in Fig.7. A 3.25 mm diameter round-ended Flag was mounted onto an XZ micrometer stage, so that it could be driven between each emitter-detector pair under test. All the LEDs in these tests were powered from a 34.8 mA constant-current supply.

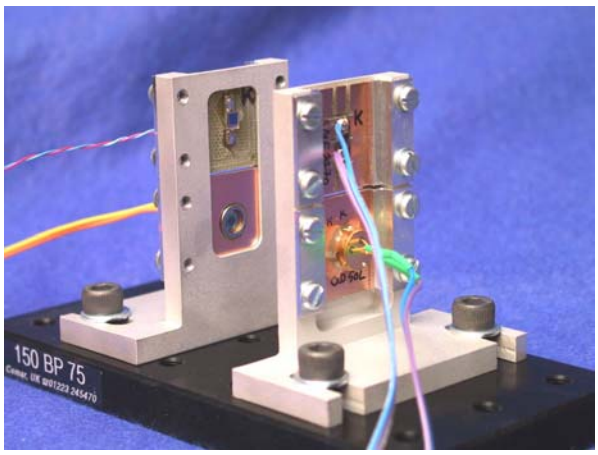

Figure 7. Shadow-sensor test jigs holding two emitter-detector pairs

Six different infrared emitter configurations were used: -

OP232 IR LED (TO-18)

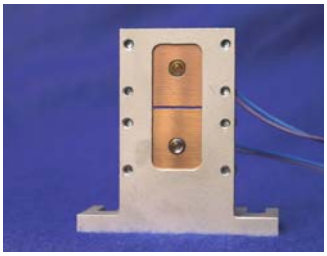

SFH480-2 IR LED (TO-18)

Dual SME2470 IR LEDs (2.6 mm separation)

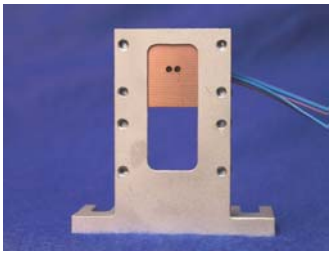

OD-880F (no photo)

SME2470 IR LED

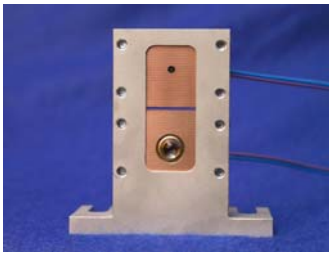

OD-50L IR LED

Five infrared photodiode detector configurations were used: -

BPW34S PD

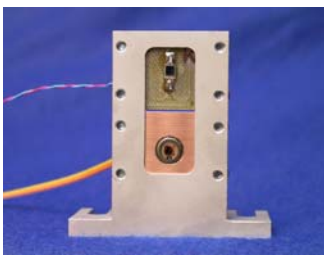

OSD5-5T PD

BPX65 (no photo)

Dual SMD2420 PDs (2.6 mm separation)

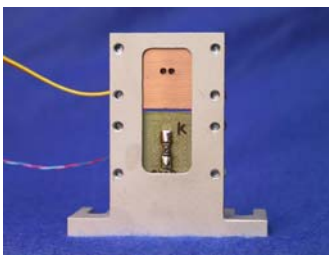

SMD2420 PD

Table 1. Infrared emitters (all were hermetically sealed packages)

Infrared LED	Package	Maximum continuous forward current (mA)	Forward voltage (V / @ mA)	Peak emission wavelength (nm)	Lens diameter (mm)	Active chip dimensions (mm)	Beam-width (1/2-angle, °)	Radiant Intensity (mW/sr @ 50 mA)
SME2470	SMT	75 (on PCB)	1.5 /50	880	1.7	*0.25 × 0.32	20	> 20 (?)
OD-50L	TO-39 (3-lead)	500	1.3 /50	880	6.35	0.76 × 0.76	7	50
OP232	TO-18	100	1.45 /50	890	3.9	—	9	25
SFH480-2	TO-18	200	1.5 /100	880	3.9	0.4 × 0.4	6 (weak annular ring at 60)	> 20
OD-880F	TO-18	100	1.55/100	880	3.9	—	3 (annular ring at 8.5)	67 (typical)

*measured from a ceramic chip with the lens removed.

Table 2. Infrared detectors

Photodiode	Package	Hermetically-sealed ?	Detection area (dimensions in mm)	Peak spectral response wavelength (nm)
SMD2420	SMT, lensed	Y	dia. (of lens) 1.7	880
BPW34S	SMT	N	2.65 × 2.65	850 (96% response at 880)
OSD5-5T	TO-5	Y	dia. 2.52	800 (96% response at 880)
BPX65	TO-18	Y	1.0 × 1.0	880

Table 3(a). Displacement sensitivity results for different shadow-sensor emitter–detector configurations

Trace #	Infrared LED emitter(s)	Photodiode detector(s)	Max. photocurrent (uA)	Full span (mm)	Max. slope (kV/m)	Noise (dBVrms/rt-Hz) @ 1 (10) Hz	Sensitivity (m/rt-Hz)	Comment
17	OP232	OSD5-5T	331	2.0	5.86	-108.787 (-120.152)	7.8e-10	Low noise, large span, good linearity
19	OD-50L	OSD5-5T	357	3 (approx.)	3.95	-109.517 (-123.127)	8.5e-10	Low noise, non-linear (two slopes), zero-offset (Flag too narrow for emitter).
13	SME2470	BPW34S (SMT)	170	1.5	7.63	-99.211 (-110.374)	1.4e-9	'Linear', good span, poor noise perf.
1	SME2470	SMD2420	19.5	0.7	17.83	-99.062 (-108.555)	6.14e-10	cf sensitivity of 2.7e-10 at 6.2 mm distance, where max slope was very similar (17.64 kV/m), and span was the same (0.7 mm). Poor noise perf.
5	2 x SME2470	SMD2420	20.9	1.6 (approx.)	5.1 (average)	-103.770 (-113.873) series connected LEDs. -104.794 (-112.062) separate LED supplies.	1.1e-9	Very non-linear. Photocurrent (split 60:40) approx 50% of expected: beaming effect too pronounced at this distance?
6	2 x SME2470	2 x SMD2420 paralleled (//)	42.8	3.2 (approx.)	2.4 (average)	-103.394 (-114.894)	2.8e-9	Very non-linear. Photocurrent approx double that of trace 5. Lower noise than trace 21
21	SME2470	2 x SMD2420 (//)	24.2	1.6 (approx.)	2.5 (average)	-97.971 (-109.888)	2.5e-9	Very non-linear. Poor noise perf.
2	OP232	SMD2420	93.8	1.4	7.6	-106.803 (-120.930)	6.04e-10	Low noise, linear, good span.

Table 3(b). Displacement sensitivity results for different shadow-sensor emitter–detector configurations

Trace #	Infrared LED emitter(s)	Photodiode detector(s)	Max. photocurrent (uA)	Full span (mm)	Max. slope (kV/m)	Noise (dBVrms/rt-Hz) @ 1 (10) Hz	Sensitivity (m/rt-Hz)	Comment
22	OD-880F	SMD2420	331	1.0	10.1	-102.087 (-112.729)	7.8e-10	Mid-noise, small span, good linearity
23	OP232	BPW34S (SMT)	542	1.9	5.61	-108.244 (-121.951)	6.9e-10	Low noise, good span, linear.
24	SFH480-2	BPW34S (SMT)	369	2.3	5.76 (4.0)	-100.557 (-115.395)	2.3e-9	Two-slopes, large span, poor noise performance.
25	OP232	BPX65	109	1.5	6.69	-107.141 (-122.477)	6.6e-10	Low-noise, good span, slightly non-linear.

Tables 3(a) and (b) show a comparison of twelve different emitter-detector pairs in terms of full-span displacement range, and displacement sensitivity. Emitter-detector pairs involving just the Honeywell devices SME2470 and SMD2420 (as used in LIGO) have been grouped together (Trace numbers 1, 5, 6, and 21), the first of these being the one used in the existing LIGO hybrid OSEM—but with an emitter-detector separation of 6.2 mm. Emitter–detector separation for these measurements was 12 mm (nominal), and the constant current through the LED(s) was 34.8 mA, in all cases. The same transconductance amplifier (based on an AD743 op-amp) was used throughout, its feedback resistor being selected for each emitter-detector pair in order to give a consistent output voltage variation of approximately 11 volts over the detection-range span. Please refer to the following two pages for the plotted traces. A ‘round-ended’ (hemispherical-ended) 3.25 mm diameter Flag was used for all of these measurements.

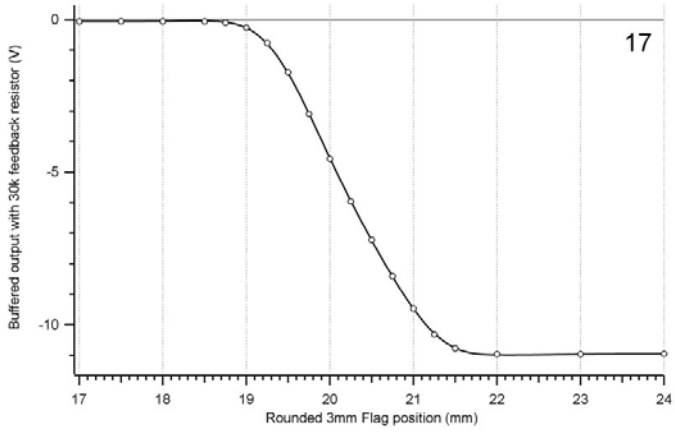
17
Buffered output with 30k feedback resistor (V)
0
-5
-10
17
18
19
20
21
22
23
24
Rounded 3mm Flag position (mm)

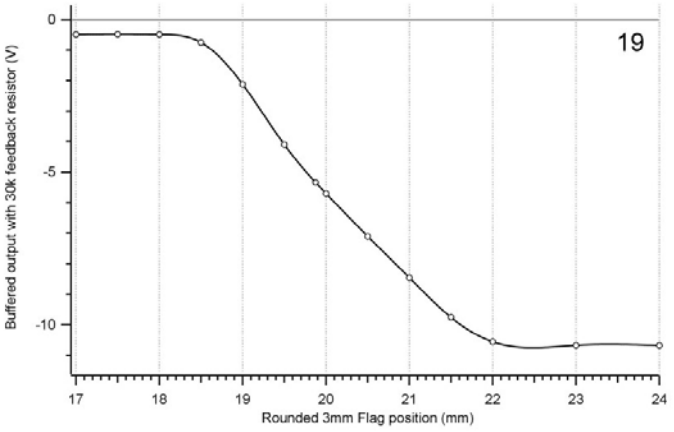
19
Buffered output with 30k feedback resistor (V)
0
-5
-10
17
18
19
20
21
22
23
24
Rounded 3mm Flag position (mm)

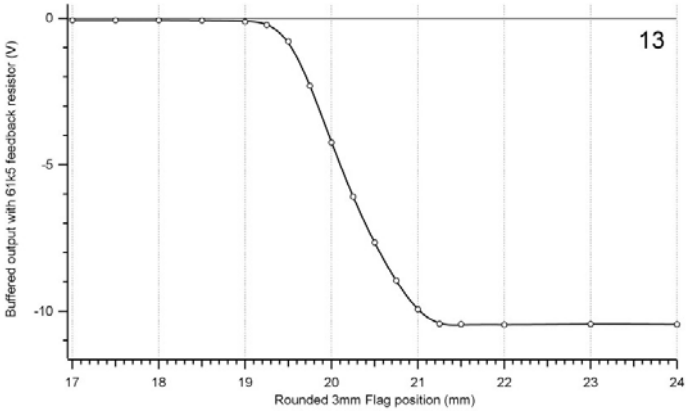
13
Buffered output with 61k5 feedback resistor (V)
0
-5
-10
17
18
19
20
21
22
23
24
Rounded 3mm Flag position (mm)

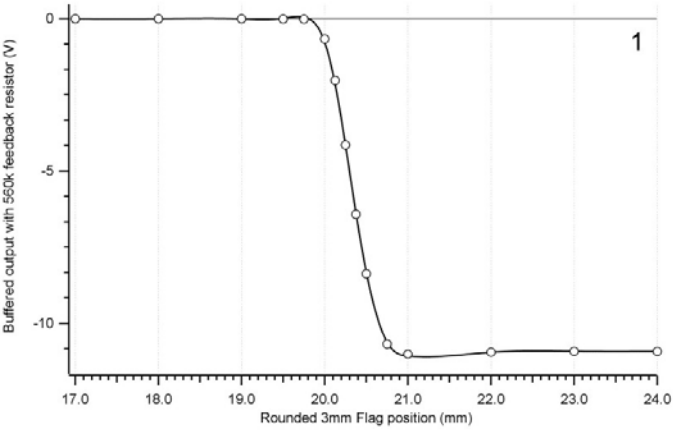
1
Buffered output with 560k feedback resistor (V)
0
-5
-10
17.0
18.0
19.0
20.0
21.0
22.0
23.0
24.0
Rounded 3mm Flag position (mm)

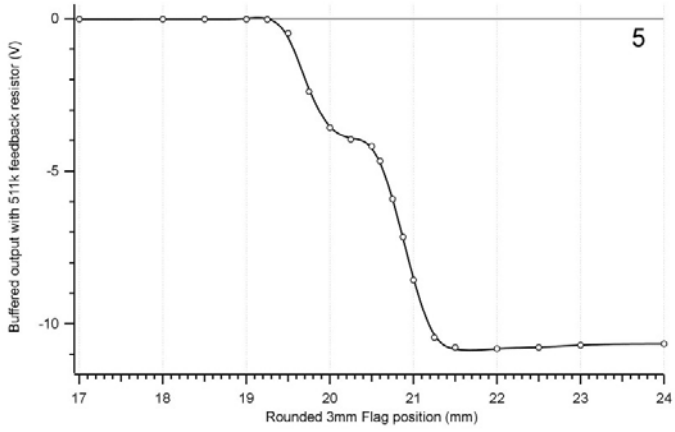
5
Buffered output with 511k feedback resistor (V)
0
-5
-10
17
18
19
20
21
22
23
24
Rounded 3mm Flag position (mm)

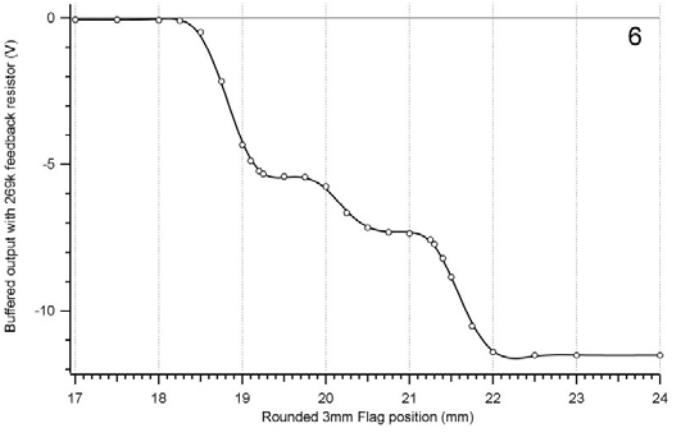
6
Buffered output with 261k feedback resistor (V)
0
-5
-10
17
18
19
20
21
22
23
24
Rounded 3mm Flag position (mm)

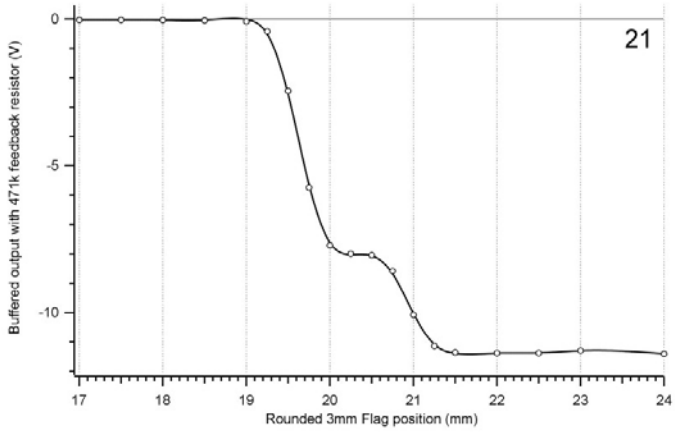
21
Buffered output with 471k feedback resistor (V)
0
-5
-10
17
18
19
20
21
22
23
24
Rounded 3mm Flag position (mm)

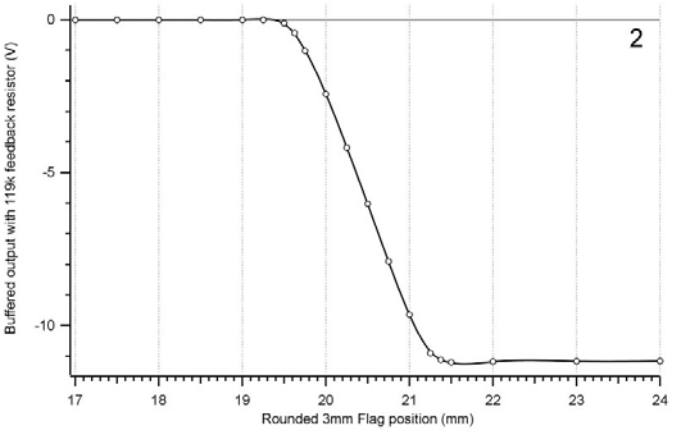
2
Buffered output with 119k feedback resistor (V)
0
-5
-10
17
18
19
20
21
22
23
24
Rounded 3mm Flag position (mm)

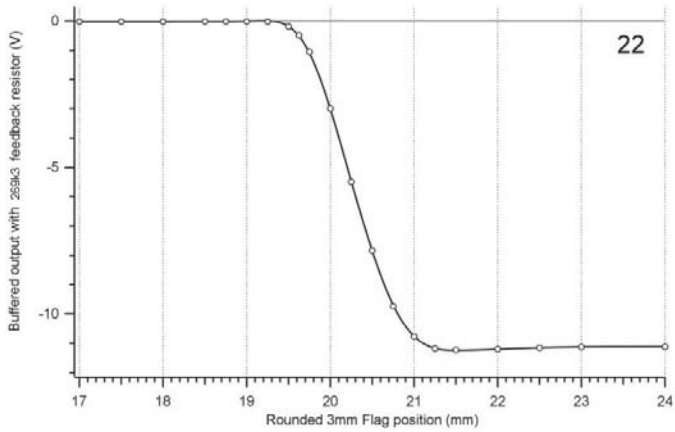
22
Buffered output with 26k3 feedback resistor (V)
0
-5
-10
17
18
19
20
21
22
23
24
Rounded 3mm Flag position (mm)

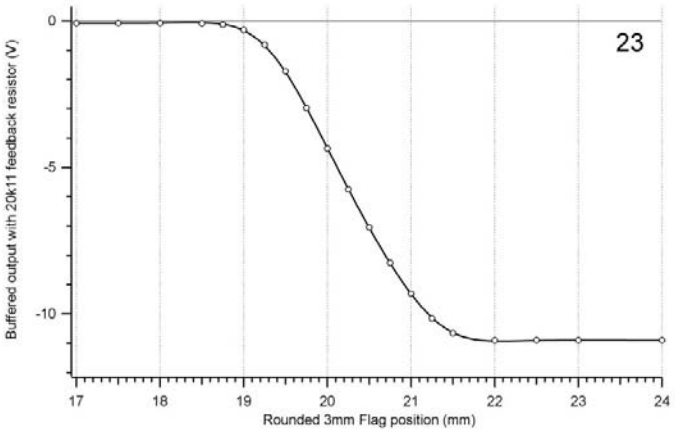
23
Buffered output with 20k11 feedback resistor (V)
0
-5
-10
17
18
19
20
21
22
23
24
Rounded 3mm Flag position (mm)

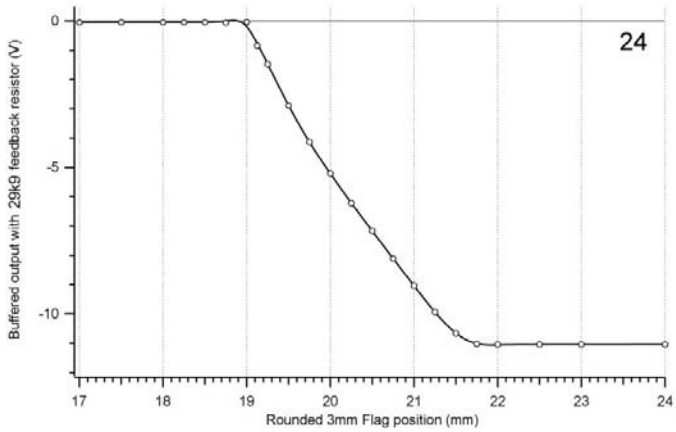
24
Buffered output with 29k9 feedback resistor (V)
0
-5
-10
17
18
19
20
21
22
23
24
Rounded 3mm Flag position (mm)

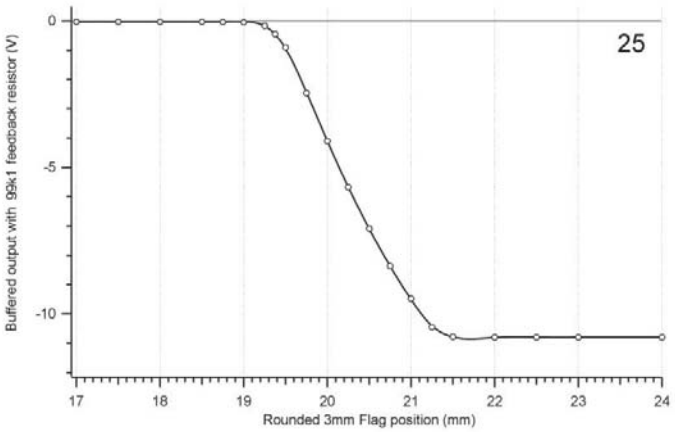
25
Buffered output with 99k1 feedback resistor (V)
0
-5
-10
17
18
19
20
21
22
23
24
Rounded 3mm Flag position (mm)

Conclusions (so far)

This report concerns work in progress, and certainly there are other devices to test beyond those mentioned here. Moreover, far from all of the device combinations in hand have been tried out, as yet. Nevertheless, some early conclusions may be drawn.

The poorest noise performances in Tables 3(a) and (b) above are all associated with the use of a single Honeywell SME2470 infrared LED emitter, as used in the LIGO hybrid OSEM. Notwithstanding this negative feature, the small diameter of this emitter, taken together with a similarly sized detector in the form of the Honeywell SMD2420 photodiode, leads to a very large slope-sensitivity for the shadow-sensor—approaching 18 kVm^{-1} (but with, unfortunately, a correspondingly small displacement span of 0.7 mm, as shown in Trace 1 above). Taken together, the noise performance and the slope-sensitivity yield a good value for the measured displacement sensitivity of approximately 3×10^{-10} m/rt-Hz, for the emitter-detector separation of 6.2 mm used in the LIGO hybrid OSEM.

However, when the emitter-detector separation was increased to approximately 12 mm, as in the work reported above, the displacement sensitivity deteriorated to 6.14×10^{-10} m/rt-Hz for the SME2470/SMD2420 pair, still with a displacement span of just 0.7 mm.

Interestingly, at this 12 mm emitter-detector separation a slightly better displacement sensitivity can be obtained by using an OP232 infrared LED in place of the SME2470 emitter. Indeed, the OP232-SMD2420 pair has a displacement sensitivity of 6.04×10^{-10} m/rt-Hz, and, while little can be made of this very slight improvement in sensitivity, what is certainly notable here is that this level of sensitivity has been achieved with a corresponding displacement span of 1.4 mm, as shown in Trace 2. This should be compared with the span of just 0.7 mm for the Honeywell SME2470/SMD2420 pair.

Also, with one exception—the OD-50L LED—the best noise performances in Tables 3(a) and (b) above are all associated with the OP232 infrared LED (from Optek Technology, Inc.).

It is now intended to re-run appropriate measurements with a shorter emitter-detector separation (approaching 6 mm), in order to see if a displacement sensitivity of 3×10^{-10} can be equalled or bettered, whilst retaining a span of greater than 0.7 mm.

N.A. Lockerbie

14 June, 2004